
Mechanically alloyed metals

H. K. D. H. Bhadeshia

Mechanical alloying involves the severe deformation of mixtures of powders until they form the most intimate of atomic solutions. Inert oxides can also be introduced to form a uniform dispersion of fine particles which strengthen the consolidated product. Large quantities of iron and nickel base alloys with unusual properties are produced commercially using this process. The theory describing the way in which the powders evolve into a solution is reviewed. There are some fundamental constraints which dictate how the microstructure must change during mechanical alloying for the process to be at all viable. The strange recrystallisation behaviour of the alloys can be understood if it is assumed that unlike normal metals, the grains in the mechanically alloyed sample are not topologically independent. Another topic discussed is the mechanical blending of microstructures containing different phases, both with and without a net reduction in free energy. MST/4799

The author is in the Department of Materials Science and Metallurgy, University of Cambridge, Pembroke Street, Cambridge CB2 3QZ, UK. Contribution to the 'Structure of materials' section of Materials Congress 2000 organised by IoM at Cirencester on 12–14 April 2000.

© 2000 IoM Communications Ltd.

Introduction

An alloy can be created without melting, by violently deforming mixtures of different powders (see Fig. 1).^{1–4} Inert oxides can, using this technique, be introduced uniformly into the microstructure. The dispersion strengthened alloyed powders are then consolidated using hot isostatic pressing and extrusion, to produce a solid with a very fine grain structure. Heat treatment then induces recrystallisation, either into a coarse columnar grain structure or into a fine, equiaxed set of grains. Columnar grains occur for two reasons: the oxide particles tend to become aligned along the extrusion direction, making that a favoured growth direction, and in the absence of particle alignment, columnar growth can be stimulated by recrystallising in a temperature gradient; the latter may be a stationary gradient or one which moves along the sample, as in zone annealing. The columnar microstructure is desirable in applications where the resistance to creep deformation is paramount.

The chemical compositions of some of the commercial alloys produced using this method are listed in Table 1. They all contain chromium and/or aluminium for corrosion and oxidation resistance, and yttrium or titanium oxides for creep strength. Yttrium oxide cannot be introduced into either iron or nickel by any method other than mechanical alloying (this was the motivation for the original work by Benjamin).¹

Microstructure

Immediately after the mechanical alloying process, the powders have a grain size which can be as fine as 10 nm locally.⁷ This is hardly surprising given the extent of the deformation during mechanical alloying, with true strains of the order of 9, equivalent to stretching a unit length by a factor of 8000. The consolidation process involves hot extrusion and rolling at temperatures of about 1000°C, which causes recrystallisation into a submicron grain size (Fig. 2). It is known that during the course of consolidation, the material may dynamically recrystallise several times.⁷ It should be emphasised that the submicron grains illustrated in Fig. 2 are not low misorientation cell structures, but true grains with large relative misorientations.⁸ Subsequent heat treatment leads to primary recrystallisation into a very

coarse grained microstructure whose dimensions may be comparable to those of the sample (Fig. 2b).

The grains in Fig. 2a are elongated because the hot rolling leaves a microstructure with a residual deformation, with a dislocation density of about 10^{15} m^{-2} (Ref. 9). Although this is large, it is not particularly high when compared with dislocation densities found in conventional steel martensitic microstructures.¹⁰ The vast majority of the stored energy of about 55 J mol^{-1} in the material is due to the very fine grain size.⁸

Chemical structure

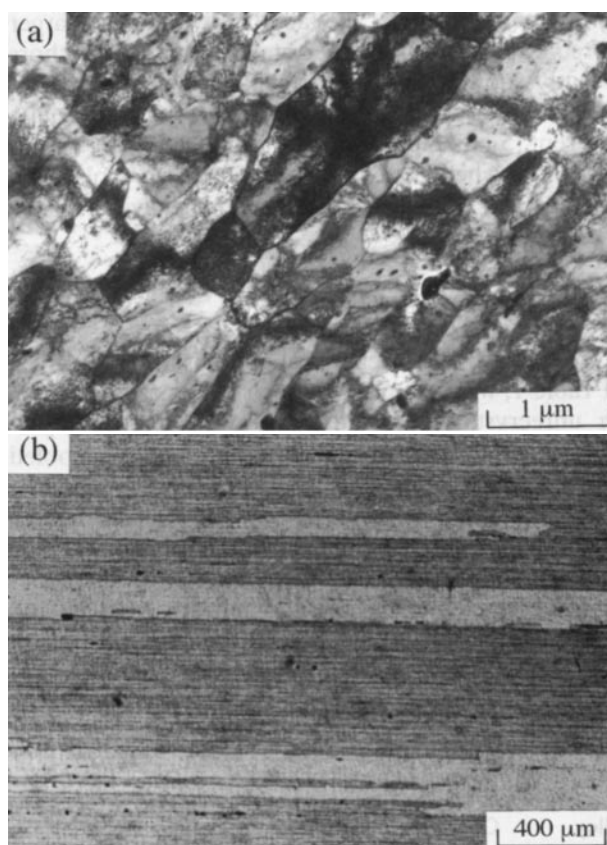
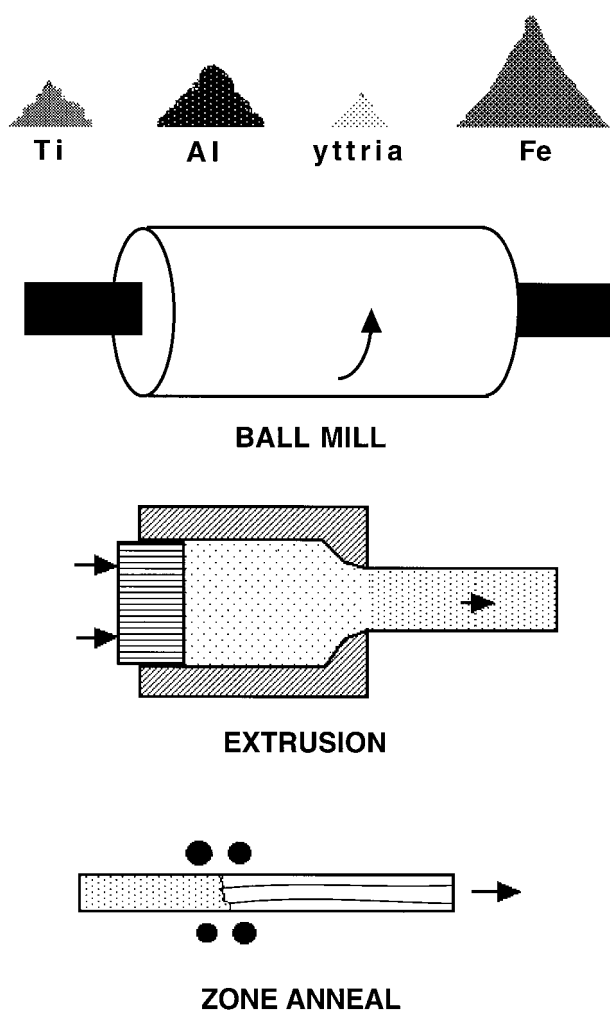
The intense deformation associated with mechanical alloying can force atoms into positions where they may not prefer to be at equilibrium. The atomic structure of solid solutions in commercially important metals formed by the mechanical alloying process has been studied using field ion microscopy and the atom probe.¹¹

A solution which is homogeneous will nevertheless exhibit concentration differences of increasing magnitude as the size of the region which is chemically analysed decreases.^{12,13} These are random fluctuations which obey the laws of stochastic processes, and represent the real distribution of atoms in the solution. These equilibrium variations cannot usually be observed directly because of the lack of spatial resolution and noise in the usual microanalytical techniques. The fluctuations only become apparent when the resolution of chemical analysis falls to less than about a thousand atoms block. The atom probe technique collects the experimental data on an atom by atom basis. The atom by atom data can be presented at any block size.

Figure 3 illustrates the variation in the iron and chromium concentrations in fifty atom blocks, of the ferrite in MA956. There are real fluctuations but further analysis is needed to show whether they are beyond what is expected in homogeneous solutions.

For a random solution, the distribution of concentrations should be binomial since the fluctuations are random (any significant deviations from the binomial distribution would indicate either the clustering of like atoms or the ordering of unlike pairs).

The frequency distribution is obtained by plotting the total number of composition blocks with a given number of atoms of a specified element against the concentration.



a TEM of section normal to extrusion direction, showing sub-micron grain structure; b optical micrograph showing coarse columnar recrystallisation grain structure resulting from heat treatment at temperatures as high as 1400°C

2 Micrographs showing grain structure of MA956

Elemental powders and master alloys/oxides milled together to produce solid solutions with uniform dispersions of oxide particles; powder is consolidated and resulting materials heat treated to achieve coarse directional grain structure

1 Stages in manufacture of mechanically alloyed metals for engineering applications

Figure 4 shows that the experimental distributions are essentially identical to the calculated binomial distributions, indicating that the solutions are random.

The atom probe data can be analysed further if it is assumed, fairly reasonably, that the successive atoms picked up by the mass spectrometer were near neighbour atoms in

the sample. Successive atoms which are identical then represent bonds between like atoms, etc., so that pair probabilities used in solid solution theory can be measured experimentally. These data can be compared against calculated pair probabilities. Thus, in a random A-B solution, the probability P_{AB} of finding A-B or B-A bonds is given by $p_{AB} = 2x_Ax_B$ where x_i is the atom fraction of element i . Similarly, $p_{AA} = x_A^2$ and $p_{BB} = x_B^2$. Table 2 shows the excellent agreement between the experimentally measured pair probabilities and those calculated assuming a random distribution of atoms.

This does not mean that the solutions are thermodynamically ideal, but rather that the alloy preparation method

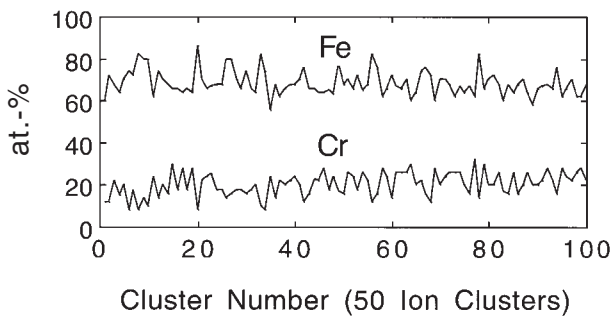
Table 1 Typical mechanical alloy compositions, wt-%

Alloy	C	Cr	Mo	Al	N	Ti	Ti ₂ O ₃	Y ₂ O ₃	Fe	W	Total O	Ni
Iron based												
MA957	0.01	14.0	0.3	...	0.012†	1.0	...	0.27	Bal.
DT2203Y05	...	13.0	1.5	2.2	...	0.5	Bal.
ODM 331	...	13.0	1.5	3.0	...	0.6	...	0.5	Bal.
ODM 751	...	16.5	1.5	4.5	...	0.6	...	0.5	Bal.
ODM 061†	...	20.0	1.5	6.0	...	0.6	...	0.5	Bal.
MA956	0.01	20.0	...	4.5	0.045†	0.5	...	0.50	Bal.
PM2000‡	<0.04	20.0	...	5.5	...	0.5	...	0.5	Bal.
PM2010‡	<0.04	20.0	...	5.5	...	0.5	...	1.0	Bal.
DT†	...	13.0	1.5	2.9	1.8	...	Bal.
DY†	...	13.0	1.5	2.2	0.9	0.5	Bal.
Nickel based												
MA6000	0.06	15.0	...	4.5	0.2	2.3	...	1.1	1.5	3.9	0.57	Bal.
MA760	0.06	19.5	...	6.0	0.3	1.0	1.2	3.4	0.6	Bal.
MA758*	0.05	30.0	...	0.3	0.6	...	0.5	0.37	Bal.
PM1000*	...	20.0	...	0.3	...	0.5	...	0.6	3.0	Bal.

*MA758 and PM1000 are without γ' strengthening.

†From Ref. 5.

‡From Ref. 6.



3 Iron and chromium concentrations of 50 atom samples of MA956

which involves intense deformation forces a random dispersal of atoms. Indeed, Fe–Cr solutions are known to deviate significantly from ideality, with a tendency for like atoms to cluster.^{14,15} Thus, it can be concluded that the alloy is in a mechanically homogenised non-equilibrium state, and that prolonged annealing at low temperatures should lead to, for example, the clustering of chromium atoms.

SOLUTION FORMATION

Normal thermodynamic theory for solutions begins with the mixing of component atoms. In mechanical alloying, however, the solution is prepared by first mixing together lumps of the components, each of which might contain many millions of identical atoms. We examine here the way in which a solution evolves from these large lumps into an intimate mixture of different kinds of atoms without the participation of diffusion or of melting.¹⁶ It will be shown later that this leads to interesting outcomes which have implications on how we interpret the mechanical alloying process.

Consider the pure components *A* and *B* with molar free energies μ_A° and μ_B° respectively. If the components are initially in the form of powders then the average free energy of such a mixture of powders is simply

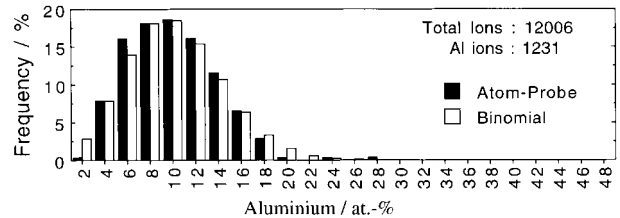
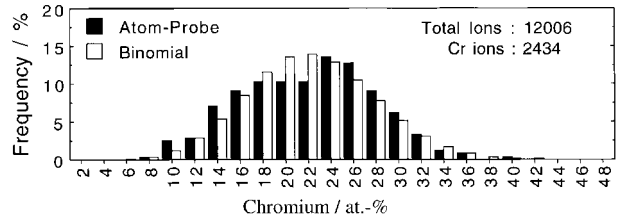
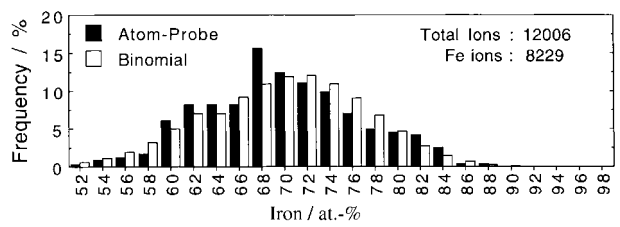
$$G(\text{mixture}) = (1-x)\mu_A^\circ + x\mu_B^\circ \dots \dots \dots (1)$$

where *x* is the mole fraction of *B*. It is assumed that the powder particles are so large that the *A* and *B* atoms do not ‘feel’ each other’s presence via interatomic forces between unlike atoms. It is also assumed that the number of ways in which the mixture of powder particles can be arranged is not sufficiently different from unity to give a significant contribution to a configurational entropy of mixing. Thus, a blend of powders which obeys equation 1 is called a mechanical mixture. It has a free energy that is simply a weighted mean of the components, as illustrated in Fig. 5a for a mean composition *x*.

In contrast to a mechanical mixture, a solution is conventionally taken to describe a mixture of atoms or molecules. There will in general be an enthalpy change associated with the change in near neighbour bonds. Because the total number of ways in which the ‘particles’ can arrange is now very large, there will always be a significant contribution from the entropy of mixing, even

Table 2 Pair probability analysis of MA956 assuming random solution: *N* total number of atoms included in analysis

Element	ρ_{AA}	ρ_{AB}	ρ_{BB}	<i>N</i>
Cr (measured)	0.638	0.324	0.038	12 168
Cr (calculated)	0.637	0.322	0.041	
Al (measured)	0.808	0.184	0.008	12 168
Al (calculated)	0.833	0.160	0.008	



4 Frequency distribution curves for iron, chromium, and aluminium in MA956

when the enthalpy of mixing is zero. The free energy of the solution is therefore different from that of the mechanical mixture, as illustrated in Fig. 5b. The difference in the free energy between these two states of the components is the free energy of mixing ΔG_M , the essential term in all thermodynamic models for solutions.

Whereas mechanical mixtures and atomic or molecular solutions are familiar in all of the natural sciences, the intermediate states have only recently been addressed.¹⁶ The problem is illustrated in Fig. 6 which shows the division of particles into ever smaller particles until an atomic solution is achieved. At what point in the size scale do these mixtures of particles begin to exhibit solution like behaviour?

To answer this question we shall assume first that there is no enthalpy of mixing. The problem then reduces to one of finding the configurational entropy of mixtures of lumps as opposed to atoms. Suppose that there are m_A atoms per powder particle of *A*, and m_B atoms per particle of *B*; the powders are then mixed in a proportion which gives an average mole fraction *x* of *B*.

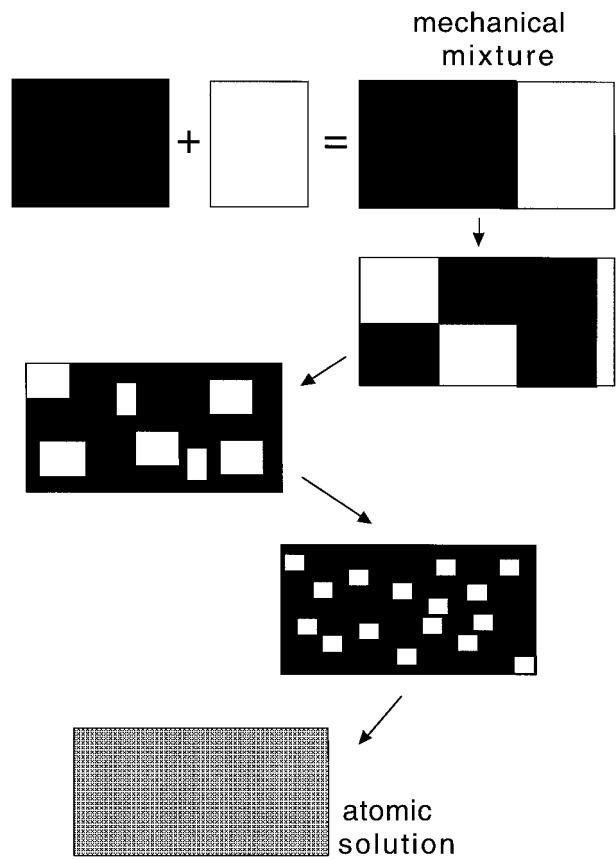
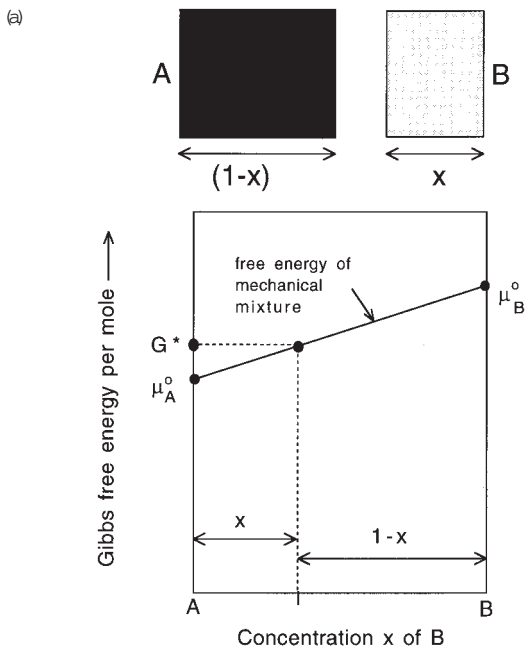
There is only one configuration when the heaps of pure powders are separate. When the powders are mixed at random, the number of possible configurations for a mole of atoms becomes

$$\frac{\{N_a[(1-x)/m_A + x/m_B]\}!}{[N_a(1-x)/m_A]! (N_ax/m_B)!} \dots \dots \dots (2)$$

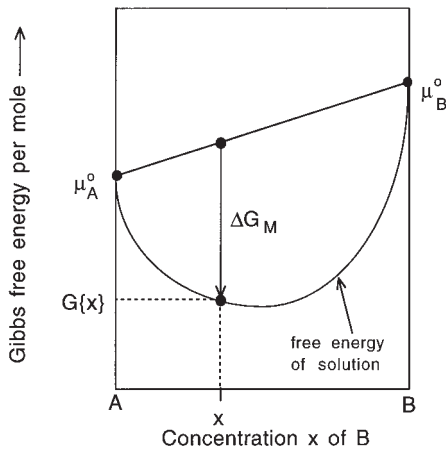
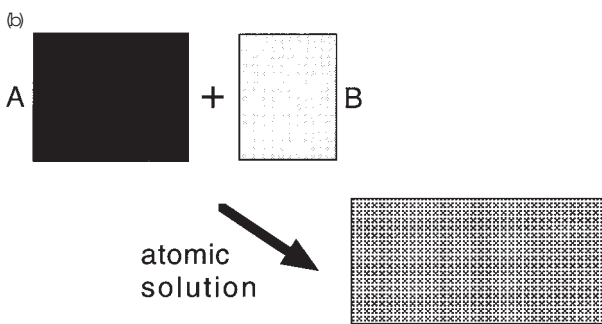
where N_a is Avogadro’s number. The numerator in equation 2 is the total number of particles and the denominator the product of the factorials of the *A* and *B* particles respectively. Using the Boltzmann equation and Stirling’s approximation, the molar entropy of mixing becomes¹⁶

$$\frac{\Delta S_M}{kN_a} = \frac{(1-x)m_B + xm_A}{m_A m_B} \times \ln \left[N_a \frac{(1-x)m_B + xm_A}{m_A m_B} \right] - \frac{1-x}{m_A} \ln \left[\frac{N_a(1-x)}{m_A} \right] - \frac{x}{m_B} \ln \left(\frac{N_ax}{m_B} \right) \quad (3)$$

subject to the condition that the number of particles



6 Illustration of evolution of an atomic solution by progressive reduction in size of different particles (process is akin to mechanical alloying)



5 Free energy of: a a mechanical mixture; b an ideal atomic solution

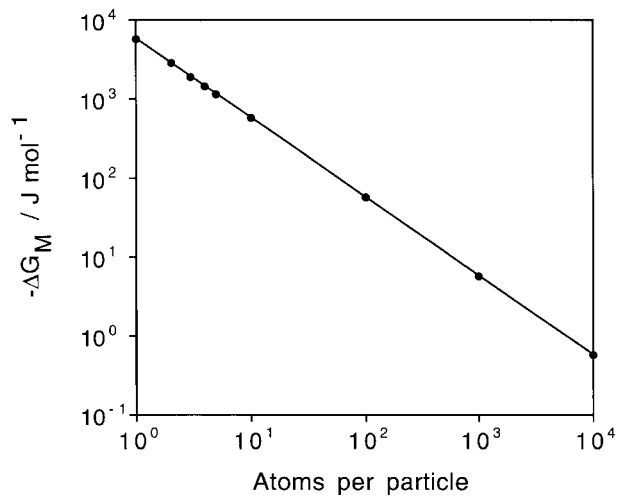
remains integral and non-zero. As a check, it is easy to show that this equation reduces to the familiar

$$\Delta S_M = -kN_a[(1-x) \ln(1-x) + x \ln(x)] \quad \dots (4)$$

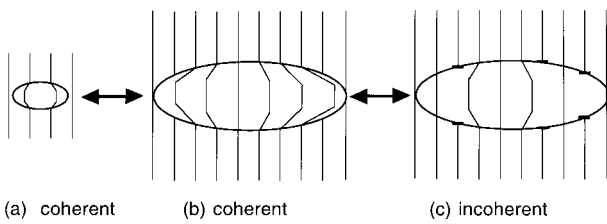
when $m_A = m_B = 1$.

Naturally, the largest reduction in free energy occurs when the particle sizes are atomic. Figure 7 shows the molar free energy of mixing for a case where the average composition is equiatomic assuming that only configurational entropy contributes to the free energy of mixing. An equiatomic composition maximises configurational entropy. When it is considered that phase changes often

occur at appreciable rates when the accompanying reduction in free energy is just 10 J mol^{-1} , Fig. 7 shows that the entropy of mixing cannot be ignored when the particle size is less than a few hundreds of atoms. In commercial practice, powder metallurgically produced particles are typically $100 \mu\text{m}$ in size, in which case the entropy of mixing can be neglected entirely, though for the case illustrated, solution like behaviour occurs when the particle size is about 10^2 atoms.



7 Molar Gibbs free energy of mixing ($\Delta G_M = -T\Delta S_M$) for a binary alloy as function of particle size: all particles are of uniform size in mixture of equiatomic average composition ($T = 1000 \text{ K}$)



8 Change in coherence as function of particle size: lines represent lattice planes which are continuous at matrix-precipitate interface during coherence but sometimes terminate in dislocations for incoherent state; precipitation occurs in sequence a-c; mechanical alloying predicted to lead to gain in coherence in sequence c-a

ENTHALPY AND INTERFACIAL ENERGY

The enthalpy of mixing will not in general be zero as was assumed above. The binding energy is the change in energy as the distance between a pair of atoms is decreased from infinity to an equilibrium separation, which for a pair of A atoms is written $-2\epsilon_{AA}$. From standard theory for atomic solutions, the molar enthalpy of mixing is given by

$$\Delta H_M \approx N_a z(1-x)xw \quad \text{where } w = \epsilon_{AA} + \epsilon_{BB} - 2\epsilon_{AB} \quad (5)$$

where z is a coordination number.

However, for particles which are not monatomic, only those atoms at the interface between the A and B particles will feel the influence of the unlike atoms. It follows that the enthalpy of mixing is not given by equation 5, but rather by

$$\Delta H_M = zN_a \omega 2\delta S_V x(1-x) \quad (6)$$

where S_V is the amount of A/B interfacial area per unit volume and 2δ is the thickness of the interface, where δ is a monolayer of atoms.

A further enthalpy contribution, which does not occur in conventional solution theory, is the structural component of

the interfacial energy per unit area, σ

$$\Delta H_I = V_m S_V \sigma \quad (7)$$

where V_m is the molar volume.

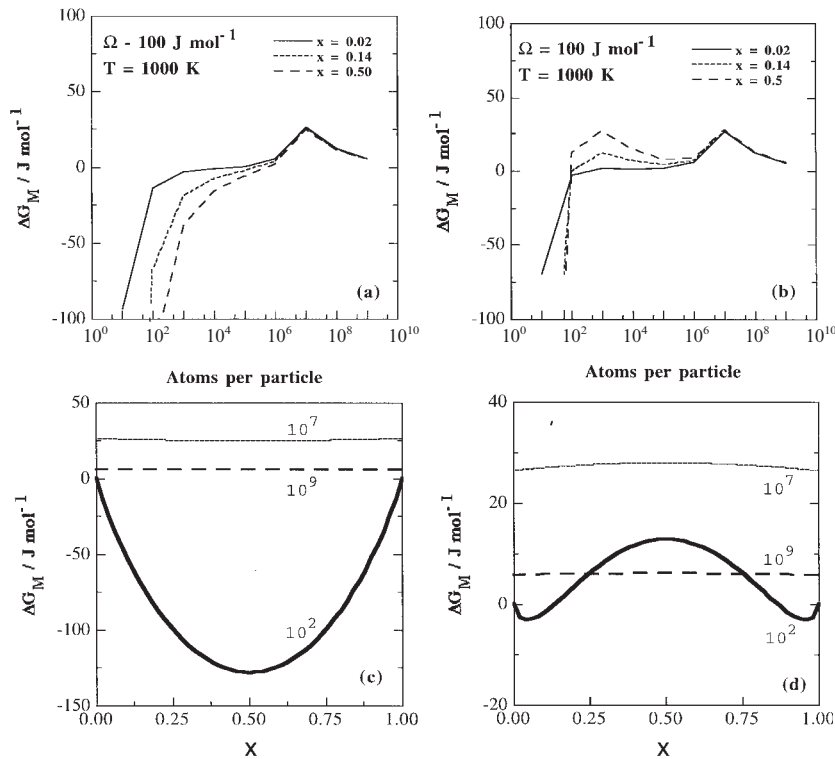
Both of these equations contain the term S_V , which increases rapidly as the inverse of the particle size m . The model predicts that solution formation is impossible because the cost due to interfaces overwhelms any gain from binding energies or entropy. And yet, solutions do form, so there must be a mechanism to reduce interfacial energy as the particles are divided. The mechanism is the reverse of that associated with precipitation (Fig. 8). A small precipitate can be coherent but the coherency strains become intolerable as it grows. Similarly, during mechanical alloying it is conceivable that the particles must gain in coherence as their size diminishes. The milling process involves fracture and welding of the attrited particles so only those interfaces which lead to coherence might succeed.

Another unexpected result is obtained on incorporating a function which allows the interfacial energy to decrease as the particle size becomes finer during mechanical alloying. Thermodynamic barriers are discovered to the formation of a solution by the mechanical alloying process (see Fig. 9).¹⁶ When the enthalpy of mixing is either zero or negative, there is a single barrier whose height depends on the competition between the reduction in free energy due to mixing and the increase in interfacial energy as the particles become finer until coherence sets in. When the atoms tend to cluster, there is a possibility of two barriers, the one at smaller size arising from the fact that atoms are being forced to mix during mechanical alloying.

The composition dependence of the barriers to solution formation becomes more clear in a plot of free energy versus chemical composition, as illustrated in Fig. 9c and d.

SHAPE OF FREE ENERGY CURVES

There are many textbooks which emphasise that free energy of mixing curves such as that illustrated in Fig. 2b must be



a negative enthalpy of mixing (unlike atoms attract); b positive enthalpy of mixing (tendency to cluster); c, d as a and b respectively but plotted against chemical composition and showing numbers of atoms per particle

9 Thermodynamic barriers to solution formation

drawn such that the slope is either $-\infty$ or $+\infty$ at $x=0$ and $x=1$ respectively. This is a straightforward result from equation 4 which shows that

$$\frac{\partial \Delta S_M}{\partial x} = -kN_a \ln\left(\frac{x}{1-x}\right) \dots \dots \dots (8)$$

so that the slope of $-T\Delta S_M$ becomes $\pm\infty$ at the extremes of concentration. Notice that at those extremes, any contribution from the enthalpy of mixing will be finite and negligible by comparison, so that the free energy of mixing curve will also have slopes of $\pm\infty$ at the vertical axes corresponding to the pure components (the intercepts at the vertical axes representing the pure components are nevertheless finite, with values μ_A° and μ_B°). It follows that the free energy of mixing of any solution from its components will at first decrease at an infinite rate.

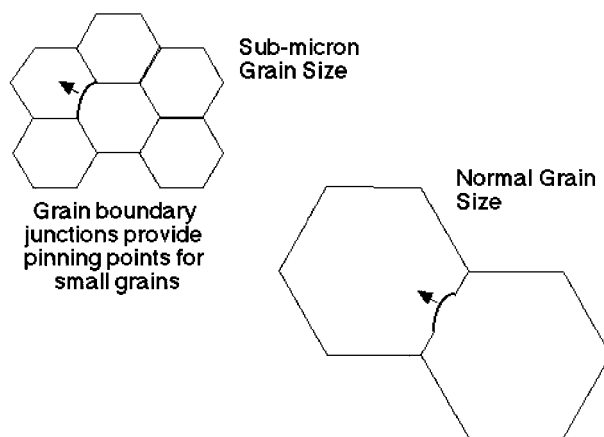
However, these conclusions are strictly valid only when the concentration is treated as a continuous variable which can be as close to zero or unity as desired. The present work emphasises that there is a discrete structure to solutions. Thus, when considering N particles, the concentration can never be less than $1/N$ since the smallest amount of solute is just one particle. The slope of the free energy curve will not therefore be $\pm\infty$ at the pure components, but rather a finite number depending on the number of particles involved in the process of solution formation. Since the concentration is not a continuous variable, the free energy 'curve' is not a curve, but is better represented by a set of straight lines connecting the discrete values of concentration that are physically possible when mixing particles. Obviously, the shape approximates a curve when the number of particles is large, as is the case for an atomic solution made of a mole of atoms. But the curve remains an approximation.

Recrystallisation temperature

One of the most intriguing features of the alloys discussed here is the fact that recrystallisation occurs at exceptionally high homologous temperatures, of the order of 0.9 of the melting temperature T_M . This contrasts with ordinary cold deformed metals which recrystallise readily at about 0.6 T_M , even though the mechanically alloyed variants contain more stored energy (Table 3).

Early work on mechanically alloyed, oxide dispersion strengthened nickel base superalloys²¹ attributed the high recrystallisation temperatures to the presence of γ' precipitates. However, there are alloys for which the γ' dissolution temperature is below that at which recrystallisation occurs.²²⁻²⁴ Furthermore, the iron base alloys do not contain any γ' and yet also recrystallise at similarly high temperatures.

It has been speculated²⁵ that recrystallisation occurs when the grain boundary mobility rises suddenly when solute drag is overcome at high temperatures. This is



10 Diagram showing nucleation of recrystallisation by formation of grain boundary bulge: this can occur with less constraint when grain junctions are spaced at distances greater than critical bulge size; grain junctions of ultrafine grains in mechanically alloyed metals are pinning points making it difficult to form large enough bulges

inconsistent with the fact that the recrystallisation temperature can be reduced by many hundreds of Kelvin by a slight additional inhomogeneous deformation.^{18,26}

The fine particles of yttrium oxide may interfere with recrystallisation but this does not explain why the limiting grain size following recrystallisation is enormous. In any case, recrystallisation is found to be insensitive to the overall pinning force.²⁷

Almost all of these difficulties are resolved when nucleation is considered in detail.^{8,27,28} It turns out that the activation energy for nucleation is very large. This is because the alloys have an unusually small grain size prior to recrystallisation. Recrystallisation nucleates by the bowing of grain boundaries, a process which for conventional alloys is straightforward since the distance between grain boundary junctions is usually larger than that between other strong pinning points. With the submicrometer grain size of mechanically alloyed metals, the grain junctions themselves act as severe pinning lines for grain boundary bowing (Fig. 10). It is easy to demonstrate that this should lead to an enormous activation energy for the nucleation of recrystallisation, many orders of magnitude larger than the activation energy associated with self-diffusion.^{8,27,28} The activation energy can be reduced dramatically if just a few grains happen to be slightly larger than others (either because adjacent grains are similarly orientated or because of local variations due to the uncertainties in the mechanical alloying process).

Blending of phase mixtures

The mechanical alloying process need not begin with powders. Microstructures which contain a mixture of phases can be deformed together until the phases blend together on an atomic scale.

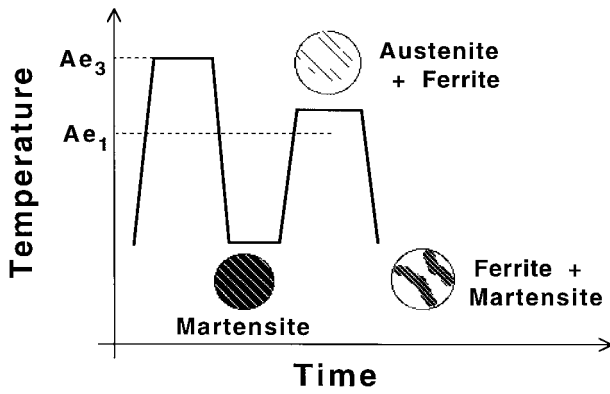
A remarkable increase in strength, from 3–5.5 GPa, has been achieved for steel wire with a microstructure entirely different from that of pearlite.²⁹ The wire, which is made by drawing, has the tradename Scifer and is currently the strongest available continuous fibre by ~ 2 GPa. The average chemical composition of the wire is Fe–0.2C–1.2Si–1.5Mn (wt-%). Although the wire is drawn in the same manner as conventional piano wire, the heat treatment is radically different (Fig. 11).

Table 3 Enthalpy of recrystallisation¹⁷⁻²⁰

Alloy	Stored energy, J g ⁻¹
MA957	1.0
MA956	0.4
MA956 sheet	≈ 0.4*
MA6000	0.6
MA760	1.0
MA758	0.3†

*Stored energy is released over relatively large range of temperatures and is difficult to measure accurately.

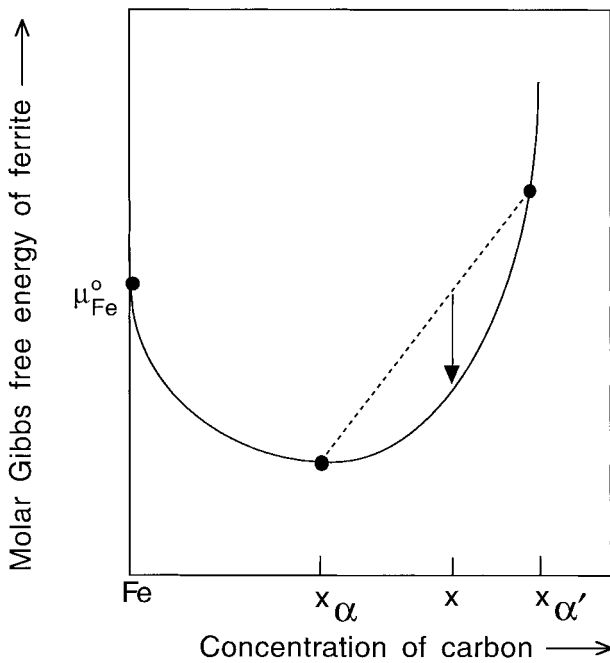
†Stored energy is small and recrystallisation occurs close to melting point making it difficult to measure.



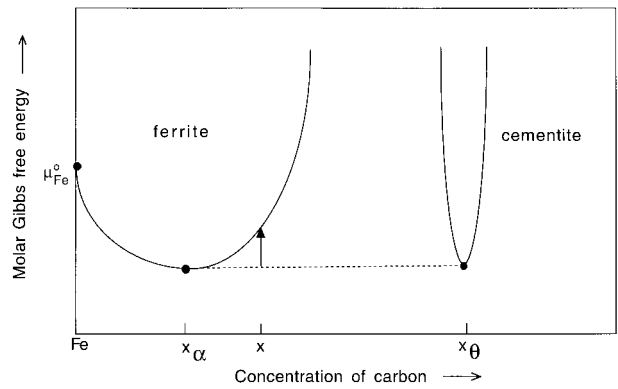
11 Heat treatment to generate mixed microstructure of ferrite and martensite before deformation

Rods of diameter 10 mm are first quenched to martensite, and then intercritically annealed in the $(\alpha+\gamma)$ phase field. This causes partial transformation into austenite which becomes enriched in carbon and manganese. The original martensite tempers to ferrite during the intercritical anneal. On quenching to ambient temperature, the layers of austenite decompose into regions of high carbon martensite containing some retained austenite. The final microstructure therefore consists of manganese rich, high carbon martensite and manganese depleted, low carbon ferrite (there may also be some cementite formed by the tempering of martensite at the intercritical annealing temperature).

The effect of the severe deformation that is used to produce Scifer is to mix the martensite and ferrite. Thus, atom probe experiments show that following the wire drawing operation, there is a great excess of carbon introduced into the ferrite.³⁰ Indeed, the high and low carbon regions in the original microstructure become mechanically blended into a relatively uniform distribution of carbon. Figure 12 shows that when the initial and final states alone are considered, without thinking about the



12 Free energy curb for ferrite as a function of carbon concentration: arrow indicates reduction in free energy



13 Free energy curves for ferrite and cementite as function of carbon concentration: arrow indicates increase in free energy

intermediate stages, there is a reduction in free energy on going from a mixture of ferrite and martensite of compositions x_α and x_α' into supersaturated ferrite with an intermediate concentration x . This is expected because the crystal structures of ferrite and martensite are essentially identical, so any difference in carbon across the microstructure amounts to a chemical heterogeneity which ordinarily would be eliminated by diffusion (diffusion can only occur if it leads to a reduction in free energy). A diffusion experiment involving large gradients of carbon in ferrite is impossible because excess carbon precipitates as cementite. Diffusion is absent during the mechanical blending of Scifer, but the material nevertheless homogenises by the deformation mechanism, with a net reduction in free energy.

Similar mechanical homogenisation occurs when mixed microstructures of ferrite and cementite are heavily deformed. Whilst the solubility of carbon in ferrite in equilibrium with cementite is very small, deformation can force the cementite to dissolve to produce supersaturated ferrite. This might happen, for example, during the intense deformation associated with the ballistic penetration of steel. The 'white layers' on pearlitic rail steels subjected to severe deformation are a consequence of mechanically induced dissolution of cementite into ferrite.³¹ Unlike Scifer, there is an increase in the free energy when an equilibrium mixture of ferrite and cementite is blended to give supersaturated ferrite (Fig. 13).

The dissolution of cementite to form supersaturated ferrite is said to occur because the cementite becomes fragmented by deformation, to a size which is below its critical nucleus dimensions from interfacial energy considerations. The proposed mechanism does not require a gain in coherence as the cementite becomes small, because the dissolution is the reverse of classical nucleation, a process reliant on diffusion and thermal fluctuations. But the alternative mechanism illustrated in Fig. 8 could lead to cementite dissolution without any need for thermal diffusion: the phases could simply be mixed mechanically. Indeed, the reduction in the free energy (equation 3) due to the larger number of fragments, would favour mixing, a term neglected in the classical explanation.

Finally, it is worth examining the magnitudes of the free energy changes associated with the sorts of mechanical alloying processes discussed in this paper. Table 4 lists the stored energies of a variety of phase mixtures in steels, relative to an equilibrium mixture of ferrite, graphite, and cementite in an ordinary steel. It is clear that the largest stored energies come from forcing atoms into phases where they would rather not be. Thus, martensitic transformation leads to the largest stored energy. By contrast, the energy stored in a mechanically alloyed ferritic steel such as MA956

Table 4 Stored energy as a function of microstructure, relative to standard state defined as mixture of ferrite, cementite, and graphite

Phase mixture in Fe-0.2C-1.5Mn (wt-%) at 300 K	Stored energy, J mol ⁻¹
Ferrite, graphite and cementite	0
Ferrite and cementite	70
Paraequilibrium ferrite and paraequilibrium cementite	385
Bainite and paraequilibrium cementite	785
Martensite	1214
Mechanical alloyed ODS metal*	55

*Iron base mechanically alloyed oxide dispersion strengthened specimen which has the highest reported stored energy prior to recrystallisation¹⁰.

is not very large in spite of the minute grain size and dislocation structure.

Summary

Commercial mechanically alloyed metals are fascinating in that they have helped reveal many new phenomena, some of which have yet to be investigated experimentally. Amongst the latter is the prediction that there is one or more barriers to the formation of a solid solution by a process in which the component particles are successively refined in size. A second prediction, which could be verified using detailed microscopy, is that there must be a gain in coherence as the mixture of powders approaches an atomic solution. One problem which appears to have been solved is the strange recrystallisation behaviour: the ultrafine and uniform grains of the starting microstructure do not behave independently and hence prevent recrystallisation until temperatures close to melting.

Severe deformation can also lead to the fragmentation and blending of phases. The process sometimes occurs in a direction which is favoured thermodynamically (as is the case with Scifer) and on other occasions where final microstructure has a higher free energy than the starting configuration. An example of the latter case is where cementite is forced to dissolve into ferrite.

Acknowledgements

I am particularly grateful to Dr Fred Hayes and Dr Rachel Thomson for organising the 'Microstructure modelling' session at the Materials Congress 2000 in Cirencester. I would also like to thank Adebayo Badmos, Carlos Capdevila, Andy Jones, and Ulrich Miller for helpful discussions over a period of many years, and Professor Alan Windle for the provision of laboratory facilities at the University of Cambridge.

References

- J. S. BENJAMIN: *Metall. Trans.*, 1970, **1**, 2943–2951.
- J. S. BENJAMIN and P. S. GILMAN: 'Metals handbook', 9th edn, 722; 1983, Materials Park, OH, ASM International.
- G. H. GESSINGER: 'Powder metallurgy of superalloys'; 1984, Sevenoaks, Butterworths.
- G. A. J. HACK: *Powder Metall.*, 1984, **27**, 73–79.
- H. REGLE: 'Alliages ferritiques 14/20% de chrome renforces par dispersion d'oxydes', PhD thesis, Université de Paris-Sud, 1994.
- P. KRAUTWASSER, A. CZYRSKA-FILEMONOWIC, M. WIDERA, and F. CARSGUHI: *Mater. Sci. Eng. A*, 1994, **A177**, 199–208.
- D. M. JAEGER and A. R. JONES: 'Materials for combined cycle power plant', Sheffield, UK, June 1991, The Institute of Materials, 1–11.
- H. K. D. H. BHADSHIA: *Mater. Sci. Eng. A*, 1997, **A223**, 64–77.
- E. A. LITTLE, D. J. MAZEY, and W. HANKS: *Scr. Metall. Mater.*, 1991, **25**, 1115–1118.
- H. K. D. H. BHADSHIA: *Mater. Sci. Forum*, 1998, **284–286**, 39–50.
- T. S. CHOU, H. K. D. H. BHADSHIA, G. MCCOLVIN, and I. C. ELLIOTT: 'Mechanical alloying for structural applications', 77–82; 1993, Materials Park, OH, ASM International.
- L. D. LANDAU and E. M. LIFSHITZ: 'Statistical physics', 344; 1958, London, Pergamon.
- K. C. RUSSELL: *Metall. Trans.*, 1971, **2**, 5–12.
- M. K. MILLER: 'Phase transformations '87', (ed. G. W. Lorimer), 39–43; 1988, London, The Institute of Metals.
- R. UEMORI, T. MUKAI, and M. TANINO: 'Phase transformations '87', (ed. G. W. Lorimer), 44–46; 1988, London, The Institute of Metals.
- A. Y. BADMOS and H. K. D. H. BHADSHIA: *Metall. Mater. Trans. A*, 1997, **28A**, 2189–2194.
- W. SHA and H. K. D. H. BHADSHIA: *Metall. Mater. Trans. A*, 1994, **25A**, 705–714.
- T. S. CHOU and H. K. D. H. BHADSHIA: *Mater. Sci. Technol.*, 1993, **9**, 890–897.
- T. S. CHOU and H. K. D. H. BHADSHIA: *Mater. Sci. Eng. A*, 1994, **A189**, 229–233.
- K. MURAKAMI, K. MINO, H. HARADA, and H. K. D. H. BHADSHIA: *Metall. Trans. A*, 1993, **24A**, 1049–1055.
- Y. G. NAKAGAWA, H. TERASHIMA, and K. MINO: 'Superalloys 1988', (ed. S. Reichman *et al.*), 81–89; 1988, Warrendale, PA, TMS-AIME.
- K. MINO, Y. G. NAKAGAWA, and A. OHTOMO: *Metall. Trans. A*, 1987, **18A**, 777.
- K. KUSUNOKI, K. SUMINO, Y. KAWASAKI, and M. YAMAZAKI: *Metall. Trans. A*, 1990, **21A**, 547.
- K. MINO, H. HARADA, H. K. D. H. BHADSHIA, and M. YAMAZAKI: *Mater. Sci. Forum*, 1992, **88–90**, 213–220.
- P. JONGENBURGER: 'ODS superalloys for gas turbines', PhD thesis no. 773, Ecole Polytechnique Federale de Lausanne, Switzerland, 1988.
- H. REGLE and A. ALAMO: *J. Phys. (France) IV*, 1993, **C7**, (3), 727–730.
- K. MURAKAMI: 'Directional recrystallisation in mechanically alloyed ODS nickel based superalloys', PhD thesis, University of Cambridge, UK, 1993.
- W. SHA and H. K. D. H. BHADSHIA: *Mater. Sci. Eng. A*, 1997, **223**, 91–98.
- Kobelco Technol. Rev.*, 1990, (8).
- H. K. D. H. BHADSHIA and H. HARADA: *Appl. Surf. Sci.*, 1993, **67**, 328–333.
- S. B. NEWCOMB and W. M. STOBBS: *Mater. Sci. Eng.*, 1984, **66**, 195–204.